Braids on the Poincaré section: A laser example

Hernán G. Solari,[1] Mario A. Natiello,[2] and Mariano Vázquez[1]
[1]*Departmento de Física, Facultad de Ciencias Exactas y Naturales, Universidad de Buenos Aires, Ciudad Universitaria, Pabellón I, 1428 Buenos Aires, Argentina*
[2]*Department of Mathematics, Royal Institute of Technology, 100 44 Stockholm, Sweden*
(Received 6 October 1995)

We discuss the topological analysis of dynamical systems represented by two-dimensional maps emphasizing the case of Poincaré maps. The central result consists in the implementation of a recent presentation of braids as deformations of circles [M. A. Natiello and H. G. Solari, J. Knot Theory Ramifications **3**, 511 (1994)] to the determination of braid types associated with periodic orbits (up to a global torsion). Since some braids imply positive topological entropy, the topological analysis can be regarded as a test of chaos. The method is specially suited for experiments where the complete reconstruction of the phase space for the flow cannot be achieved at a reasonable cost. We apply these ideas to data sets produced in a laser physics experiment for which the reconstruction of the phase space of the flow is nearly impossible. [S1063-651X(96)03309-0]

PACS number(s): 05.45.b+, 42.65.Sf, 47.20.Ky

I. INTRODUCTION

The computation of the periodic orbits which are present in an experimental data set is a central tool in assessing the topological behavior of the system. In the case of three-dimensional (3D) systems, periodic orbit organization can be turned into a strong tool for the analysis of data. First, the presence of certain periodic orbits implies that the associated (2D) Poincaré map has positive topological entropy [1], thus being a relatively simple and certain test for chaos [2]. Second, the linking between periodic orbits and the way they rotate around each other along the flow, characterized by the linking number [3] and the relative rotation rate [4], are strong indicators of the organization of the flow, since as long as two periodic orbits exist (i.e., for values of the system parameters away from bifurcations affecting these orbits) their linking will be invariant. Small errors in the determination of the orbits will not alter their relative linking.

These indicators can be summarized in a template [5]. A template is a branched manifold containing information about the periodic orbits present in the attractor of the system together with their relative linking and rotation rates. The experimental data can provide only a finite number of periodic orbits and a template can be induced from them using the linking and folding information of the orbits [6]. The periodic orbits present in the system might be different from those present in the induced template in two ways. First, there might be orbits in the template that are not present in the system. Second, there might be orbits in the system not present in the template since the data set may lack information about periodic orbits from some regions of the phase space not visited by the attractor. The induced template is an educated guess (conjecture) about the behavior of the system; its appeal comes from the ability of organizing the information in a simple, integrated, form.

When a flow can be imbedded in three-dimensions and in addition it admits a Poincaré section, its periodic orbits are described by their braid type [7]. The existence of a Poincaré control section imposes strong restrictions to the flow. Continuity and differentiability of the flow reflect themselves in the continuity and differentiability of the Poincaré first-return map. Moreover, most properties of the flow, including the above mentioned linking numbers, relative rotation rates, and topological entropy, are coded in the braid type and can be read directly on the Poincaré section.

The topological organization of the periodic orbits can be used as a test for theoretical models. Any acceptable model will have to present the same topological organization of the periodic orbits as the observed data. It can be shown [8] that the maps of the disk preserving a (set of) periodic orbit(s) can be classified, allowing for change of coordinates and deformations, by the braid type of the orbit(s). This is to say that the necessary condition for a theoretical Poincaré map of the disk to be acceptable as a model for a data set is to have the same braid types as the data set for the periodic orbits ''present'' in the data.

Until now, all computations of periodic orbits required a good reconstruction of the flow. This reconstruction is not always possible in practice, as in the motivating example of this work which is a laser with saturable absorber. Our time-series is a recording of the intensity of the laser. When the intensity drops very close to or below the detection threshold, the experimental error renders it very difficult and even impossible to reconstruct the flow in that region of phase space. This difficulty calls for finding new ways to characterize periodic orbits which do not need to imbed the data set in order to produce a model flow.

In a previous article [9] we proved that the braid type associated to periodic orbits in 3D flows can be determined *directly* from the Poincaré section. This is particularly appealing from the applications point of view because it suggests that the efforts in modeling experimental data can be focused in the Poincaré section rather than in the flow. Once one has established by some means that a data set could be imbedded in three dimensions, it suffices to have a good description of the Poincaré map in order to understand the topological organization of the periodic orbits hidden in the data. One does not actually need to perform the imbedding. In this way, the difficulties encountered with our motivating example led to the development of alternative and more

powerful mathematical tools to analyze 3D flows admitting a Poincaré section.

In this paper we review the theory associated with determining braid types associated with periodic orbits on the Poincaré section in Sec. II. The reader may want to move directly to Sec. III, where we discuss a method to model the Poincaré first-return map and to analyze periodic orbits, and use Sec. II as a reference section. In Sec. IV we present an application to the laser system. Conclusions and future views are in Sec. V.

II. THEORETICAL BACKGROUND

Using the parametrization in time we can regard periodic orbits in 3D flows as smooth closed nonintersecting curves in 3-space. They can be described by their knot type [10], or more interestingly by a braid [11], using explicitly the additional orbit invariant induced by the existence of a Poincaré section, namely the period. In this section we will discuss why periodic orbits are interesting to understand the topological organization of a flow, what is the braid group, how it is related to periodic orbits, and how to compute the braid information of a periodic orbit directly from the Poincaré section.

A. Why periodic orbits?

Our ultimate goal is to assess if a given data set is ''chaotic,'' i.e., if it arises from a dynamical system running in the chaotic regime. By ''chaotic'' we mean a system having positive topological entropy [2].

Topological entropy, intuitively, measures the way a flow stretches and folds into itself by way of the time evolution. A minimal physical requirement is that the time evolution should be continuous and with continuous inverse. In the specific case of this paper (3D flows admitting a Poincaré section) this translates into having a Poincaré map which is continuous and with continuous inverse (i.e., a homeomorphism).

The role of periodic orbits in this game is the following. If one happens to establish that a particular periodic orbit is present in a data set, and therefore infer that this orbit is a possible solution of the underlying dynamical system, the rate of stretching and folding of the flow has to be compatible with the existence of this orbit, because of the continuity assumptions. Intuitively, if one has certain very twisted orbits, the whole flow has to be highly twisted. We conclude that the existence of certain periodic orbits will imply positive entropy and hence chaoticity. A more precise statement in terms of the braid associated to a periodic orbit is given below.

B. Periodic orbits and braids

Consider a period-n orbit on a 3D flow. Its intersection with the Poincaré section will consist of n different points on the 2D Poincaré surface. For the sake of simplicity we can consider this surface to be a topological disk in $\mathbb{R}^2$. A period-3 orbit is depicted in Fig. 1(A), where the intersection of the orbit with the Poincaré section is indicated with black dots.

In order to describe the orbit we can consider the evolution of all n points simultaneously during one period starting and finishing on the chosen Poincaré surface. Each point will develop a ''thread'' along the evolution, arriving finally to some other point (among the n points of the orbit). We illustrate this description in Fig. 1(B).

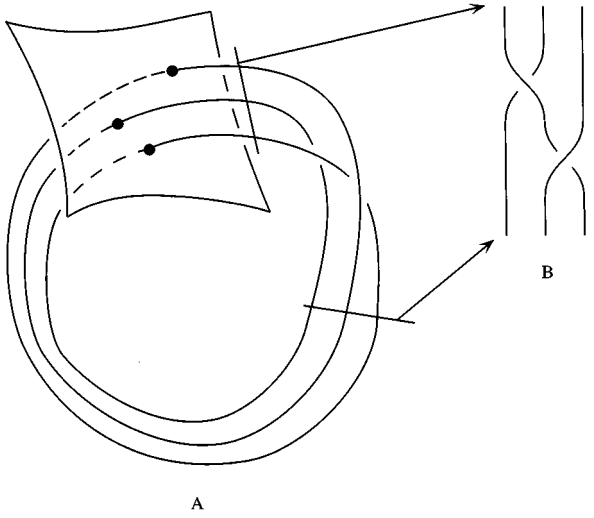

FIG. 1. (A) A period-3 orbit. The black dots denote the intersection of the orbit with a control section. (B) The braid representative of the orbit.

More precisely, the threads can be parametrized by a function $f:[0,1]\mapsto(\mathbb{R}^2)^n$, where $f(t)$ consists of n different points of the disk describing the location of the threads at time t. It is clear from Fig. 1 that $f(1)$ is just a permutation of $f(0)$ since we can take them to be the same set of points on the same control section. Moreover, since the orbit cannot intersect itself, no two entries in $f(t)$ can coincide, so we can more accurately replace the image space by $X_n=(\mathbb{R}^2)^n-\Delta$, where Δ is the great diagonal in $(\mathbb{R}^2)^n$, i.e., $(x_1,\ldots,x_n)\in\Delta\Leftrightarrow x_i=x_j$ for some $i\neq j$. We end up describing the orbits by functions $f:[0,1]\mapsto X_n$, where $f(0)$ is a permutation of $f(1)$ and n characterizes the period. Since the labeling of the initial points $(x_1,\ldots,x_n)$ is arbitrary we should not distinguish the function $(x_1,\ldots,x_n)(t)$ from $(x_{p_1},\ldots,x_{p_n})$, where $n\mapsto p_n$ is a permutation. This is achieved identifying the points $(x_1,\ldots,x_n)$ and $(x_{p_1},\ldots,x_{p_n})$ for all possible permutations, i.e., the space X_n is further replaced by X_n/S_n, where S_n stands for the permutation group of n elements.

In order to characterize the way an orbit tangles to itself we have to gain independence with respect to changes of coordinates that would only change the appearance of the orbit. Moreover, if we are to make sense of statements such as ''the orbit exists in the parameter region $\ldots$'' we have to allow for continuous deformations of the orbits. Hence it makes sense to classify orbits up to homotopies. (Two maps $f,g:A\rightarrow B$ are said to be homotopic if they can be continuously deformed into one another [12].)

We can then consider the equivalence classes with respect to homotopies of the functions $f:[0,1]\mapsto X_n/S_n$, where now $f(1)=f(0)$ since we have identified points in X_n that differ in a permutation. Each orbit will belong to one and only one equivalence class, so the classes are representative of the

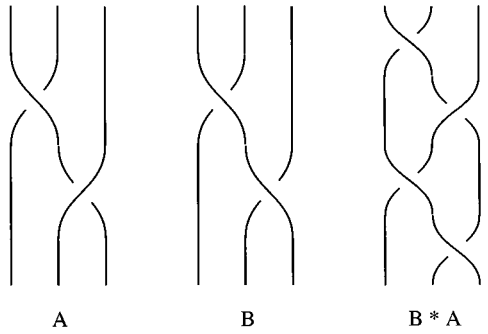

FIG. 2. A pictorial representation of the multiplication operation of the braid group.

orbit structure. These classes are the elements of the *braid group* B_n, [13] also called the *fundamental group* $\pi_1(X_n/S_n)$.

C. Braids

Figure 1(B) is a pictorial representation of a braid. We can define a braid multiplication as is shown pictorially in Fig. 2, simply by appending one braid to the other.

Braids can be described enumerating the crossings among the n threads. Each elementary crossing is called a (free group) *generator* σ_i [13]. Consecutive threads can cross in two possible ways. Conventionally we call σ_i the crossing where thread i goes *over* thread $i+1$. The generator σ_i^{-1} describes the alternative possibility ($i+1$ over i). It is clear that σ_i^{-1} is the inverse of σ_i with respect to the multiplication defined above. Just by ''pulling tight'' the involved threads one sees that $\sigma_i\sigma_i^{-1}=1$. This pictorial description of braid multiplication and inverse generators may convince the reader that braids actually form a group. A rigorous demonstration can be found in [13].

Enumerating the minimal number of necessary generators in their order of appearance, each braid has an associated *braid word*. The braids of Fig. 2 have the words $A=\sigma_2^{-1}\sigma_1$, $B=\sigma_2\sigma_1$, and $C=\sigma_2\sigma_1\sigma_2^{-1}\sigma_1$, where we agree on writing the generators from right to left (hence, the top crossing is at the right end of the word). With this convention, group multiplication amounts to formal multiplication of the braid words, i.e., $C=BA$.

Note that although it can be useful to retain the identity of a thread all along the braid, the numbering of the generators in the braid word assumes that after each crossing the threads are renumbered starting from the left.

We note that the generators of the braid group satisfy two constitutive relations, namely $\sigma_i\sigma_{i+1}\sigma_i=\sigma_{i+1}\sigma_i\sigma_{i+1}$ and $\sigma_i\sigma_j=\sigma_j\sigma_i$ when $|i-j|>1$. These relations also have a nice interpretation in terms of thread-diagrams and ''pulling tight'' as above.

D. Braid conjugation

Concerning the relation between braids and periodic orbits, it is apparent that the choice of Poincaré section can alter the associated braid word. Choosing the section ''ahead'' in the direction of the flow, the crossings that were originally at the beginning of the word (occurring first in the direction of the flow) will be moved to the end of the word. Hence, the same orbit can be described by different words. We show an example in Fig. 3. The different words are related by a conjugation operation,

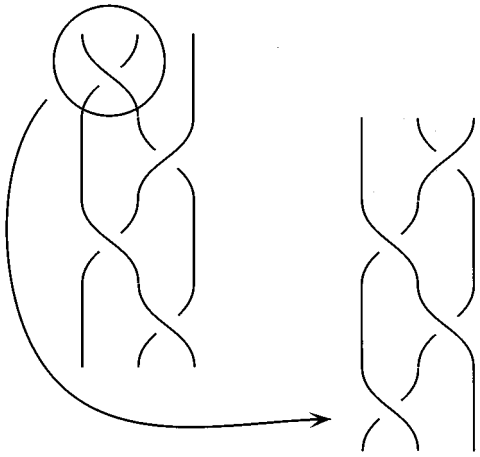

FIG. 3. Braid conjugation. The first crossing on the left picture goes into the last crossing on the right picture. The direction of the flow is downwards.

$$R_W b = b L_W, \quad R_W = b L_W b^{-1}, \tag{1}$$

where L_W, R_W describe the words associated to the conjugated braids, with the convention that all terms of the form $\sigma_i^{-1}\sigma_i$ can be canceled out of a braid word. In the case of Fig. 3, L_W, R_W indicate the left and right braids, respectively, and $b=\sigma_1$.

In general we can say that braid words related by a conjugation convey the same information. Moreover, it can be shown that conjugation is an equivalence relation, and hence it is preferable from the periodic-orbit viewpoint to work directly with the equivalence classes of braids with respect to conjugation.

E. Braids in the Poincaré section

Braids can be described graphically directly on the Poincaré section, without resorting to the flow in order to ''read'' the crossings of the threads [9]. In this subsection, we will sketch the procedure for attaining this description.

There is one piece of information from the periodic orbits that is lost when going to the Poincaré surface. In fact, the association between flows and Poincaré first-return maps is many-to-one. If the flow as a whole has a global torsion (i.e., it rotates as a whole around the flowing axis) which is an integer number times 2π, the first-return map remains unaltered. We will call these integer rotations a *full torsion* or a *full twist*. A flow compatible with a Poincaré map is called a *suspension*. A given Poincaré map admits many suspensions which differ from each other in the number of full twists.

The full twists constitute a subgroup Z_n of the braid group B_n. They are in fact the *center* of this group, i.e., those elements that commute with all elements of B_n [9]. Hence the quotient group B_n/Z_n is the relevant entity to characterize periodic orbits of any flow having a given first-return map. We will in the sequel refer only to this quotient group.

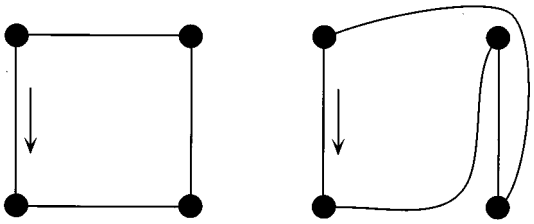

FIG. 4. Braids on the Poincaré surface: Two circles belonging to different homotopy classes.

Consider the n periodic points on a Poincaré section corresponding to a periodic orbit of a flow. We consider $n>1$ in the sequel. Draw a topological circle joining the points of the orbit with arcs on the Poincaré section. There are many ways to produce a circle connecting nonintersecting arcs among the points. One can classify all these ways by homotopy classes. Two circles are equivalent if they can be deformed into each other without moving the periodic points. The different equivalence classes label the inequivalent ways of constructing circles. In Fig. 4 we show two inequivalent circles on a period-4 orbit.

How are these circles related to periodic orbits? Choose one circle as a starting point. This includes choosing an ordering of the periodic points along the circle. Now ''slide'' the circle along the flow until it returns to the control section as described in Fig. 5. It is reasonable to expect that the transformed circle will contain some information related to the braid of the orbit.

The relevant result [9] is that the equivalence classes of circles is in one-to-one correspondence with the quotient group between the braid group and the full torsions.

Hence, we can obtain a representation of the braid generators σ_i and further of the braids directly on the Poincaré surface. Taking Fig. 4(a) to represent the starting point (and hence the identity braid), Fig. 4(b) represents the generator σ_2. This generator can be conceived as a ''turn'' where one takes two periodic points on the Poincaré surface and switches them clockwise, together with the arc joining the points. Inverse generators are represented by counterclockwise turns.

Using this method, the braid of a periodic orbit can be read directly on the Poincaré section. The whole recipe is summarized in Fig. 5. First, draw a circle joining the points of the orbit in a given sequence. The image of this circle by the Poincaré map will be a twisted circle inequivalent (in general) to the original one. A representative of the braid of the orbit can be obtained by reading the turns required to deform the original circle into the final one.

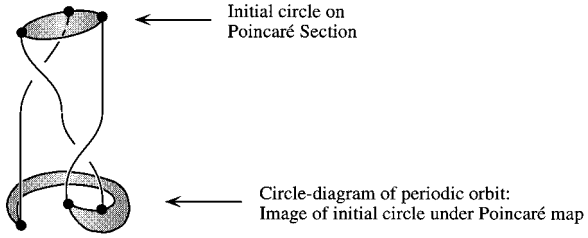

FIG. 5. Braids on the Poincaré surface: The image of the starting circle by the Poincaré map.

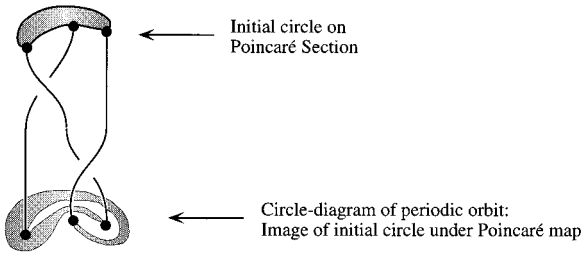

FIG. 6. Braids on the Poincaré surface: A different starting circle gives a conjugate braid.

F. Braid type

If we are not going to privilege one suspension of the map in front of another, or one Poincaré section in front of an equivalent one, we will have to identify several braids with the same orbit. Two braids will be considered equivalent, say $\beta\equiv\alpha$, in the sense that they possibly label the same periodic orbit, if they differ by a number of full twists or a conjugation,

$$\gamma^{-1}\beta z^m\gamma=\gamma^{-1}\beta\gamma z^m=\alpha, \tag{2}$$

where $z=(\sigma_1\sigma_2\cdots\sigma_{p-1})^p$ is the braid representative of a full twist of the braids with p strands.

It is straightforward to verify that we have defined an equivalence relation which classifies the braids into different inequivalent classes. The *braid types* are precisely these classes, i.e., two braids have the same braid type if they are related by a conjugation and a number, m, of full twists.

Let us review now the form in which we associate a braid with the periodic orbit(s) of a map. First, we draw a circle connecting all the periodic points of the periodic orbits(s) being considered and take the image by the map of the circle obtaining a new one (inequivalent to the original in general). We then read off the name of the braid in terms of the generators of the braid group that need to be applied to deform the original circle (we shall call it the identity) into its image.

There is clearly one degree of arbitrariness in this procedure: the choice of original circle is absolutely arbitrary. What would happen if we pick a different (inequivalent) identity? What does the i actually mean in σ_i ?

The generator σ_i exchanges the i and $i+1$ points along the original circle. Changing the circle is then equivalent to giving a different meaning to the generator. Consider two different choices of circles C_1 and C_2; let α be the braid that acting on C_1 produces C_2 and let β_i be the braid associated to the map as is read from the action of the map on C_i. We would like to know the relation between β_1 and β_2.

If we call σ_i the generators as read with C_1 and Σ_i as read with C_2, we find that $\Sigma_i=\alpha\sigma_i\alpha^{-1}$. That is, we first put C_2 in the form of C_1, next exchange i and $i+1$ applying σ_i, and finally send back C_1 to C_2. It follows immediately that any product of Σ's is transformed in the same form, thus $\beta_2=\alpha\beta_1\alpha^{-1}$. The conclusion is that the choice of original circle does not affect the braid type. This reasoning is illustrated in Fig. 6.

Now consider two choices of Poincaré section, Π_1 and Π_2, such that the second lies ahead of the first along the flow. The action of the flow on the identity C_1 of the first section is the circle $\beta_1 C_1$. While going from Π_1 to Π_2, the identity deforms to $C_2 = dC_1$. Let us take C_2 as the identity on Π_2. The action of the flow on C_2 can be described by $d\beta_1 d^{-1} C_2$. Pictorially, we flow backwards from C_2 on Π_2 to $d^{-1}C_2 = C_1$ on Π_1. We act with the flow, returning to $\beta_1 d^{-1} C_2$ on Π_1, and finally we flow forward again to Π_2. Figure 3 was prepared having this example in mind.

Notice the parallel between the two situations described above. In both cases, the conclusion is that changing the arbitrarily chosen ''identity'' circle the Poincaré map generates conjugated braid names, hence we read exactly the same braid type.

G. Braids in higher dimensions

The essential geometric property that is underlying the structure of periodic orbits of 2D maps is the fact that the fundamental group of the punctured disk ($D^2 - \{0\}$, i.e., the disk without one of its interior points) is nontrivial. In simpler words, closed curves can be distinguished by their (signed) number of turns around the puncture. Curves having a different number of turns cannot be deformed continuously into one another. Similarly, the braids of n strands are related to the fundamental group of the disk with n punctures.

Going over to higher dimensions the fundamental groups become trivial. A famous consequence of this is the fact that all knots are trivial in four or more dimensions.

This result is of a fundamental nature in the sense that general physical systems are described by partial differential equations. Regarded as ODE's (ordinary differential equations), physical systems should be of very high and often infinite dimension. How then is it possible that from *experimental results* originated in a high-dimensional system one obtains linked periodic orbits, an object which is characteristic of 3D flows? There is a simple answer to this question when low-dimensional models can be regarded as the center manifold reduction of high-dimensional physical systems.

A dynamical system admitting a Poincaré section of dimension $k > 2$ can in certain cases still be associated to braids [9]. The condition is that the Poincaré map has $k-2$ strongly contracting directions, i.e., that its dynamics can be essentially described by a 2D map, namely the map on the 2D center manifold, irrespective of the dimension $k+1 > 3$ of the original flow. The fundamental group of the periodic orbits of the whole system dressed with their strongly stable directions equals the fundamental group of the periodic orbits on the center manifold, i.e., the braid types. Proof of these results can be found in [9].

H. Braids that imply positive entropy

An important result of Boyland [1] states that for *irreducible* braid types there is a simple test for positive topological entropy. Following Katok [2] positive topological entropy is a way of assessing that the system is *chaotic*. Let us recall the procedure step by step.

An irreducible braid type can be intuitively described as one that cannot be decomposed in smaller independent subsets. In particular, an n-threaded braid describing a period-n orbit with n a prime number is always irreducible [1]. We will focus further on this particular case.

The existence of certain orbits in 2D diffeomorphisms requires a high degree of stretching and folding of the domain. In particular, the existence of a *pseudo-Anosov* orbit [1] implies the existence of infinitely many other orbits and of positive topological entropy.

A test for positive topological entropy is, hence, to determine if a system has a periodic orbit with a braid of pseudo-Anosov type. The result by Boyland states that if a braid is irreducible, then the exponent-sum, i.e., the sum of the exponents of the generators associated to the braid word, can be used as a test for entropy. If the exponent sum is not an integer multiple of $n-1$, the braid is pseudo-Anosov. In the negative case there is still a chance. If β^n, i.e., the nth power of the braid, is not homotopic to a rotation, then the braid β is of pseudo-Anosov type.

III. THE METHOD

As mentioned in the Introduction, the motivating example of this work is time-series from a laser system. When the intensity recorded in the time-series drops to values very close to or below the detection threshold, the experimental error renders it very difficult and even impossible to properly reconstruct the flow in that region of phase space. One way out of the problem, then, is to give up the reconstruction of the flow and attempt to reconstruct the Poincaré map instead.

A sample of a time-series is shown in Fig. 7 showing that there are large periods of zero or very low intensity in between high-intensity peaks. Our main working hypothesis is that each peak can be regarded as a point on a Poincaré surface of the system, and hence the time-series records how the system jumps from one peak to the next, i.e., how it moves on the Poincaré surface, as dictated by the Poincaré map.

To describe each peak we would like to use as much information as possible from the part of the time-series well above the detection threshold, while avoiding as much as possible the ''dead times'' between consecutive peaks. If the description is successful, we will have a good model of the Poincaré map instead of a poorer model of the original flow.

A. Peak description

To identify each peak we consider n consecutive points of the time-series (in our computations $n=5$) to determine whether there is a local maximum among those points. A cutoff value c disregards maxima which have too low absolute intensity. The peak is further represented by p points to each side of the local maximum. The amount of points p was taken as one-half of the largest interpeak distance after ignoring the ''zero intensity'' segments of the data (i.e., where the intensity drops below a threshold value t, so that it can be assumed to have reached ''zero level''). This choice of p guarantees that all data points above ''zero intensity'' will participate in the identification of the peaks (eventually with some overlap). The sampling interval was taken identical to the experimental sampling. However, sampled points were interpolated so that the peaks coincide with the $p+1$ sample avoiding in this form adding one spurious dimension to the reconstructed data. Both the threshold and the cutoff were

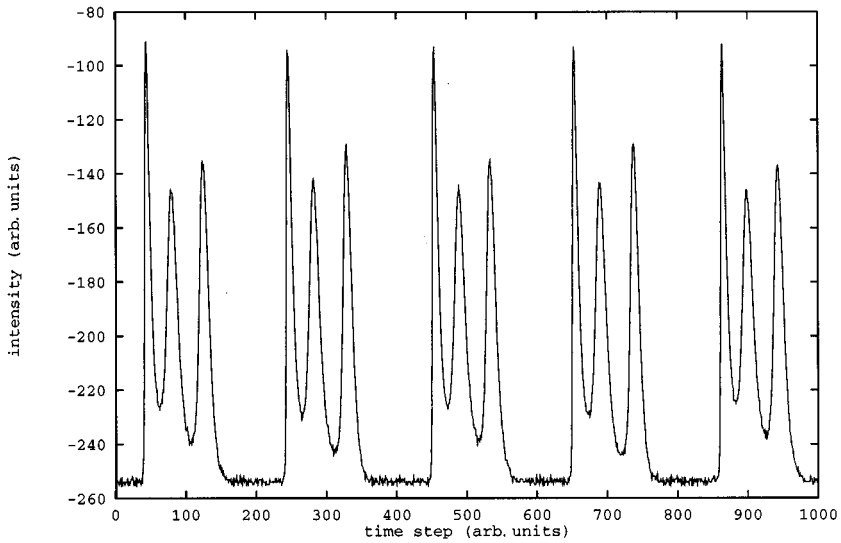

FIG. 7. A piece of a time-series for the laser experiment.

chosen a few percent above the absolute minimum of the time-series. Typical values were $p\sim 20$, $c\sim 3\%$, $t\sim 0.5\%$. In order to have a more confident characterization of each peak we used a $(2p+2)$-dimensional array where apart from the $2p+1$ consecutive points of the time series we added a ''coordinate'' containing the interpeak distance, which can be regarded as a measure of the ''dead time'' region. As a consequence of our procedure, the time-series is recasted as a set of N consecutive points in a $(2p+2)$-dimensional space (where N corresponds to the number of peaks above cutoff) describing a Poincaré map.

Since we are interested in characterizing the variations in the data from peak to peak, we first subtracted the average-peak vector from each peak array. This can be regarded as a coordinate shift in the $(2p+2)$-dimensional peak space which eliminates all offsets due to the experimental setup, leaving only the differences between peaks (plus eventual experimental and measuring errors) as relevant information.

B. Model Poincaré map

In order to separate the most relevant components in peak space we used a standard method known as the principal components analysis [14,15]. It can also be regarded as a case of biorthogonal decomposition [16] since each peak has associated $2p+2$ ''spatial'' coordinates and we decompose the peaks in terms of linearly uncorrelated ''spatial modes.'' The outer product of each peak vector is used to compute the matrix

$$A=\sum_{i=1}^{N} v_i v_i^T . \tag{3}$$

A is symmetric and positive semidefinite, providing therefore a test for the quality of our computation: No eigenvalue of A should be negative. Moreover, the eigenvalues of A can be interpreted as follows. If all vectors v_i were equal, A would have only one nonzero eigenvalue of size $\lambda=N|v|^2$. If we assume that all entries are built of a single vector v_i plus a random error of size ϵ, we will obtain one eigenvalue of large size and all other eigenvalues of size ϵ. We can in general say that large eigenvalues contain information about the system while small eigenvalues carry the noise and other sources of error. The associated eigenvectors thus yield a way to characterize relevant coordinates.

We finally proceed to project the $(2p+2)$-dimensional imbedding space into its d first coordinates where d is the imbedding dimension of the points in the Poincaré section. For low dimensional imbeddings (one or two) the dimension can be usually recognized by inspection of the data set. Alternatively we introduce a criterion based in the false-neighbors method [17,18]. The procedure is as follows.

(i) Order the coordinates according to the size of the eigenvalues.

(ii) Fix the size of a box as a few times the noise-to-signal ratio, B, times the range of the first coordinate, Γ. In our case we take $B=0.06$, however the computation is not too sensitive to this choice.

(iii) Let $F(i)$ be the fraction of false neighbors that can be recognized using the first i-coordinates and box-length B. We will consider d to be the dimension of the imbedding space if d is the smallest integer such that $F(d)$ is greater than a certain tolerance, Q (in our case $Q=0.95$). In other words, we take the imbedding dimension as the smallest number of coordinates that allow us to resolve a $100\times Q$ percent of the false neighbors.

This procedure is statistical in nature and as such leaves open the possibility of having statistically negligible regions (''measure zero'' regions) where $d+n$ dimensions, $n>0$, are needed to describe the data (think for example of a manifold in the shape of the figure eight that would require an imbedding dimension of two according to our procedure but requires at least three dimensions at one point). The topological analysis does not tolerate these sorts of situations and demands a true (proper) imbedding of the attractor. It is therefore necessary to further check and probably fine tune the embedding resulting from the above procedure before performing any actual computation.

Projecting the peaks onto the eigendirections associated to the largest eigenvalues of A, we produce a model of the

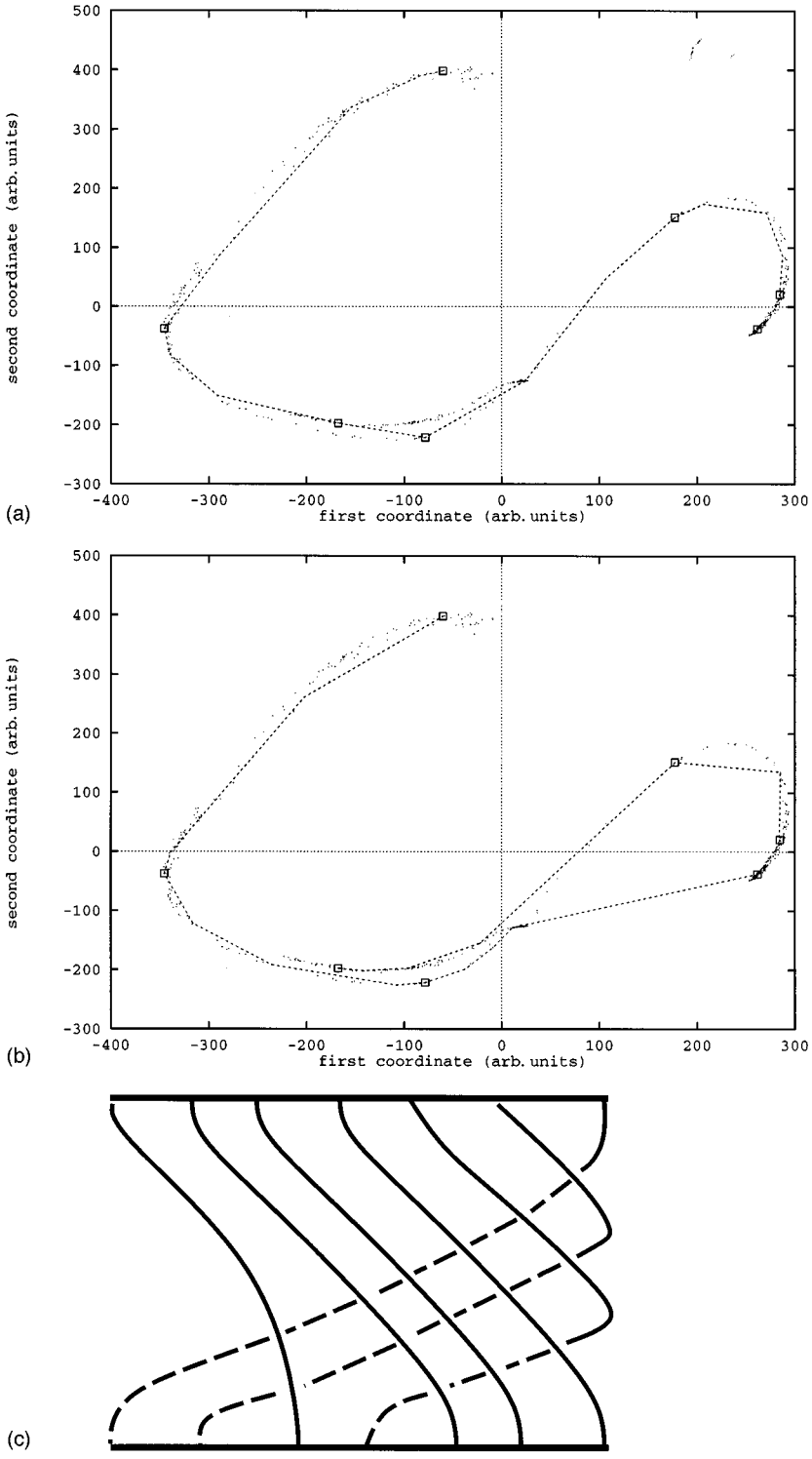

FIG. 8. A period-7 orbit of the laser experiment. (a) The orbit on the Poincaré surface. (b) The image of the model circle. (c) The associated braid.

Poincaré map of the system. The new coordinates are called z_i, where i labels the eigenvalues in descending order. In our motivating examples the imbedding dimension was either one (in one case) or two (two cases). The Poincaré surface is described by the coordinates z_1 and z_2+z_3 yield a branched curve as the locus of the Poincaré map. The choice of z_2+z_3 as second coordinate rather than simply z_2 satisfies the need of removing ''measure zero'' self-intersections of the attractor.

The identification of segments of data closely resembling the periodic orbits was done using the method of close returns [19,6]. Essentially, the idea is that if a sufficiently large piece of the time-series is almost repeated after some interval, we can consider that the points in the interval belong to—or are close to—a periodic orbit (after finishing the orbit, the system repeats itself). The repetition occurs only approximately and under a limited period of time due, among other causes, to the unstable character of the periodic orbits em-

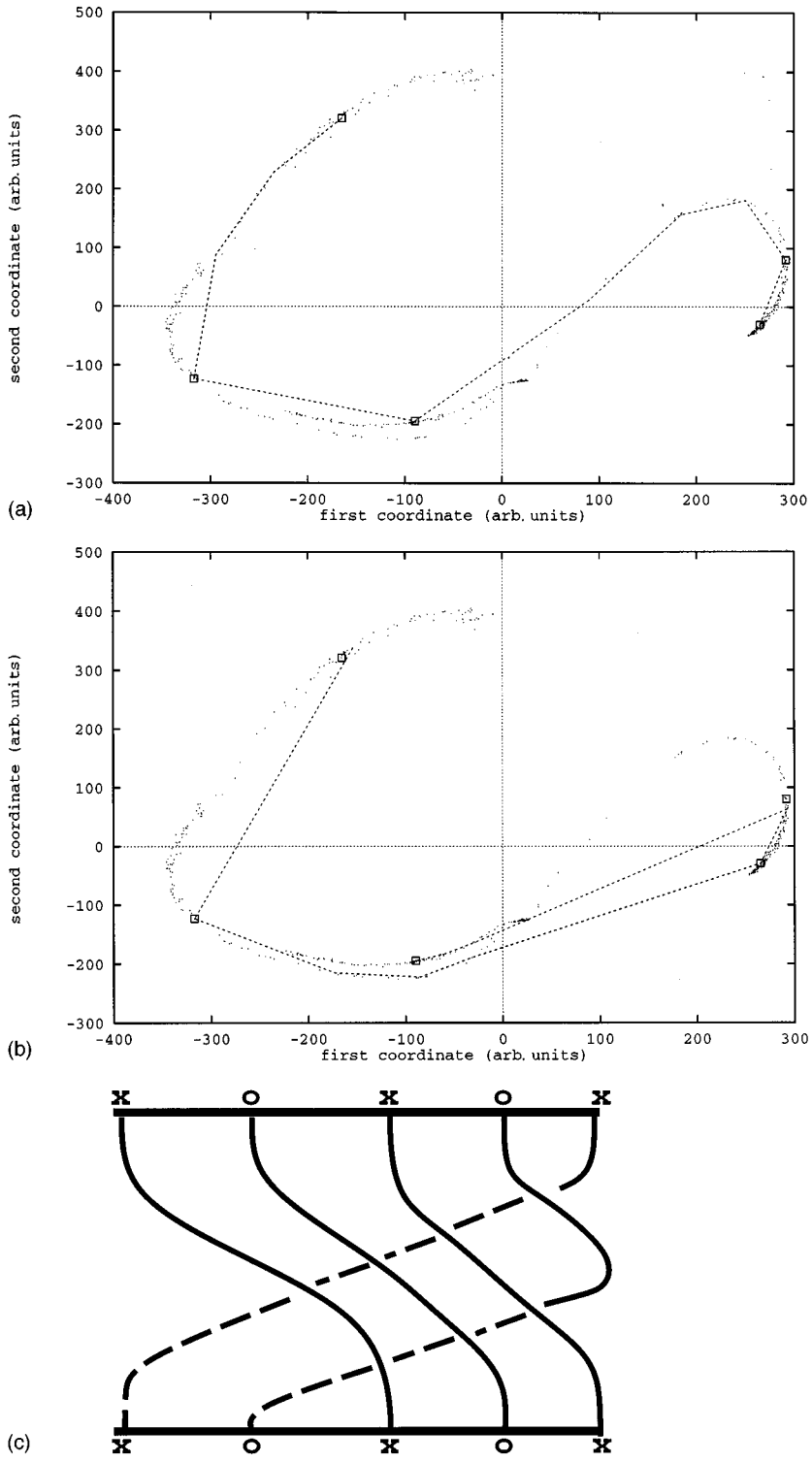

FIG. 9. A period-2 and a period-3 orbits of the laser experiment. (a) The orbits on the Poincaré surface. (b) The image of the model circle. (c) The associated braid.

bedded in a strange attractor. We have that if

$$\delta = \frac{1}{M}\sum_{j=0}^{M-1} |x_{l+j} - x_{k+j}| < \epsilon, \tag{4}$$

then the segment between points l and k is a close representative of a periodic orbit. Typically ϵ is a few percent of the standard deviation of the data and M is several times the peak width $2p+1$. Note that the identification of periodic orbits is performed without reference to the imbedding or the Poincaré section. We first locate the periodic orbit and later find the intersection of the orbit with the chosen Poincaré section.

In general, one obtains many candidates for each periodic orbit. In the applications, we have systematically chosen those with lowest δ as orbit representatives. More precisely,

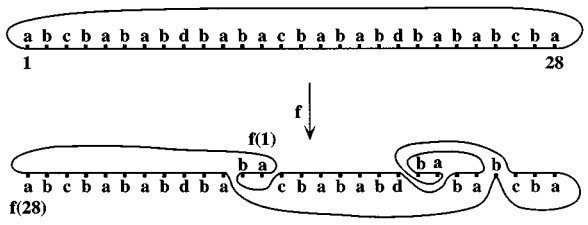

FIG. 10. Pictorial representation of the braid associated to the link of four orbits, of periods 10(a), 13(b), 3(c), and 2(d), present in one data file.

we have applied the following recipe.

(i) We consider only data segments that begin at a peak, thus avoiding having several copies of the same orbit shifted in time.

(ii) Points are interpolated. This avoids distorting the closeness of a return with the mismatch between periods and sampling times.

(iii) For each initial point we find the final point that produces the smallest δ. The segment is disregarded if $\delta > \epsilon$. This criterion avoids n successive close returns of period P being confused with a period nP.

(iv) No data segment can be used to represent more than one orbit. In case of conflict only the orbit with the smallest δ is accepted. That criterion complements the previous one. This is, even if the segment beginning at x_i has its closest return, say $\delta_i < \epsilon$, in the segment beginning at x_{i+P}, we proceed to disregard $\{x_i \cdots x_{i+P}\}$ as representative of a periodic orbit if it has a subsegment with a close return smaller than δ_i.

In Fig. 8(a) we show a period-7 orbit identified on the Poincaré surface.

The rest of the method is a simple procedure. (a) Draw a circle joining the points of the candidate orbits using other close-lying points on the Poincaré surface. (b) Compute the image of the circle by the model Poincaré map. (c) Read the braid type associated to the orbit by disentangling the image of the circle obtained in (b).

IV. APPLICATIONS

As an example of the identification procedure we read the braids of a period-2 plus period-3 link, a period-7 orbit (Fig. 8), and a period-13 orbit. The period 7 was present in three of the studied data sets while the period 13 was present in two data sets. In all cases the topological circle (a smooth closed curve without self-intersections) required by the method is obtained closing the dotted line joining the periodic points with a suitable arc going from point n to point 1.

In Fig. 9(a) we show the period-2 and period-3 orbits displayed in the Poincaré surface. Figure 9(b) displays the image of the model circle by the Poincaré map, while Fig. 9(c) shows the associated 5-threaded braid.

The associated braid can be described in terms of the elementary generators. Recall that the process to read the braid is just to apply the generators to the initial circle [Fig. 9(a)] until the final circle [Fig. 9(b)] is obtained. The generators are written right to left in order of application. The *braid word* is then 2341234 where each digit i represents a generator σ_i. The braid is clearly reducible into a 2- and a 3-threaded subunit. Both subunits and also the whole 5-braid have only positive generators. The linking number between the subunits is 2. The computation of the linking number from the braid is straightforward. It amounts to one-half of the number of signed crossings of the threads of the 3-subunit with those of the 2-subunit. Moreover, since the braid has only positive generators all crossings have sign $+1$. The above result is obtained verifying that there are in total four crossings.

This 5-threaded link is compatible with a horseshoe template [6]. With this we mean that both orbits or equivalently both braid types are present among the (infinitely many) horseshoe orbits. Moreover, the linking between both orbits in our data is also the same as the one obtained from the horseshoe representatives.

Concerning the period-7 orbit of Fig. 8 the results are more interesting. The braid can be read as 45623456123456 and it is irreducible, since it corresponds to a prime-period orbit [1]. The braid also has positive generators only, and it corresponds to the horseshoe period-7 orbit with permutation (3567421). Using 0 and 1 for the orientation preserving and orientation reversing branches of the horseshoe template the period 7 is identified by the word $00101x1$ (''x'' denotes either 0 or 1, since the horseshoe orbits 0010101 and 0010111 are homotopic). Moreover, the braid has associated positive entropy since the exponent-sum is 14, which is not divisible by $6 = 7 - 1$ (actually the entropy is 0.476818 [20]). Hence, the orbit is of pseudo-Anosov type, which allows us to determine that the data set comes from a chaotic system.

In Fig. 10 we present the braid including all the periodic orbits detected in one of the data files and their word in pictorial form.

Our last example is the period-13 orbit, which is the orbit of the largest period among those shown in Fig. 10. In Fig. 11 we can see the attractor in the model Poincaré section and the construction that produces the braid name. The permutation associated to the orbit reads (5689$abcd$74321) (using hexadecimal numbering) while, with the same convention used before, the braid reads (789abc)(456789abc) (3456789abc)(23456789abc)(123456789abc), which is again a horseshoe orbit with horseshoe name $00101010010x1$ (again the letter x stands for 1 or 0 since both situations are indistinguishable in this context).

Note that in this case there is some arbitrariness in the way we connect points belonging to the two leaves of the attractor. Referring to Fig. 11 we see that whether we connect the points 5-6-7 (beginning to count at the upper left corner and following the lines) in this order, as 5-7-6 or as 7-5-6, is just a question of taste. Actually, if a different choice is made the braid name will change to a conjugated braid [9].

In the case of the period-13, the exponent sum is $48 = 4 \times (13 - 1)$. In order to decide on the basis of Boyland's theorem whether this braid has associated a positive topological entropy, one has to compute the 13th iteration of the braid and determine if it is homotopic to a rotation.

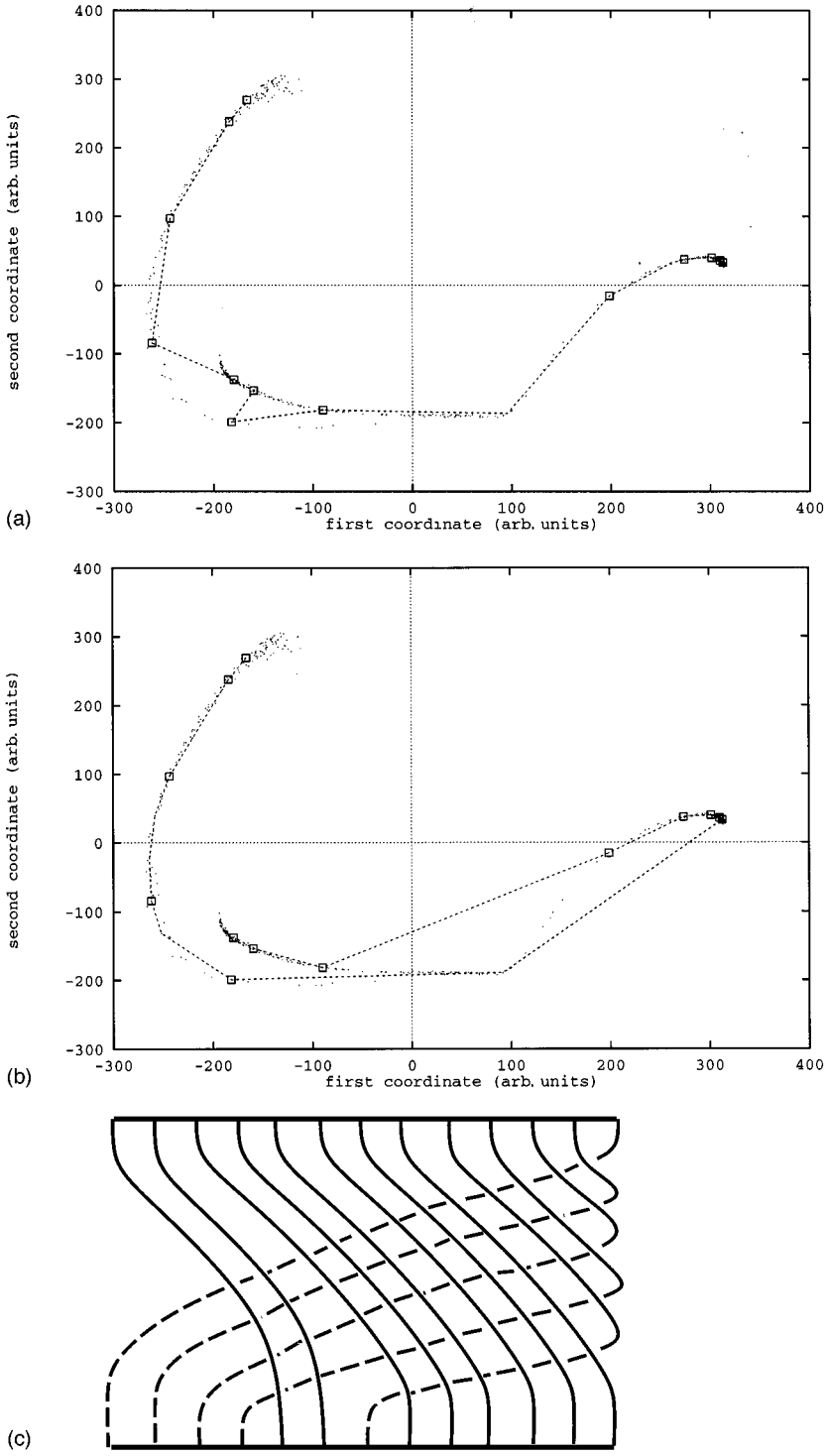

FIG. 11. Strange attractor in Poincaré section and period-13 orbit. (a) The attractor. (b) The first image of the attractor. (c) The braid associated to the orbit (points marked with *x* and *o* belong to the two different branches).

V. CONCLUSIONS AND FURTHER VIEWS

The association between periodic orbits of 3D systems admitting a Poincaré section and braid types can be performed modeling the Poincaré map directly instead of modeling the flow [9]. This paper is an implementation and exemplification of this result, using data sets from a laser experiment that rendered very difficult to produce a 3D imbedding of the flow.

We have shown that the modeled Poincaré map is compatible with a Smale horseshoe, by which we mean that all the periodic orbit representatives extracted from the data sets exist in the Smale horseshoe and are organized in the same form in the laser system and in the horseshoe. This result is consistent with previous work in laser data sets where chaotic motion was also associated to a horseshoe [4,21].

The study of the experimental data sets presented in this work has been performed trying to make use of all the information available in the sets. This includes finding represen-

tatives of the periodic orbits without references to any particular imbedding and choosing the imbedding such that all the temporal data sets can be reconstructed from the variables of the imbedding.

The procedure presented in this work requires finding the image by the map of a topological circle connecting the points belonging to the periodic orbits. For a densely sampled (constructed) phase space linear interpolation using sampled points is enough, as in the present case. However, for other data systems there might be a need to use more advanced techniques such as tesselations.

We must emphasize that the methods presented here are suited for all maps of the two-dimensional disk (D^2). The application of the method to problems imbedded in other two-dimensional surfaces might not be straightforward since the description of the braids depends on the topology of the phase space.

A final word must be devoted to the problem of imbedding. Topological analysis is done on imbedded data. One should more properly say that the analysis describes *both* the experimental system *and* the imbedding [22]. More precisely, for any two imbeddings of the data that can be extended to an imbedding of a (deformed, topological) disk the braid type of the periodic orbits will remain unchanged because of the very definitions of imbedding and braid type. It is precisely the possibility of performing such an extension of the imbedding that is the key of the discussion in [22].

The method presented in this work cannot go beyond certain intrinsic restrictions. The problems basically arise because any reconstruction of a map based on finite (in size and precision) experimental data represents an extrapolation. We are making a hypothesis on the behavior of the map both for the observed points and for those points (a measure-one set) where we have no experimental information. There is also some degree of arbitrariness in the procedure. For example, the determination of the imbedding dimension is done on the basis of statistical estimations, such as the false-neighbors method we implemented in this paper. These estimations are not sharp, in the sense that they do not give a yes or no answer, but yield instead a measure of how meaningful a result may be. Moreover, the estimation relies on the *reasonability* of several choices such as, e.g., the size of the partition boxes. Too big boxes have too many points inside for any dimension. Too small boxes are in general empty or have (occasionally) only one point.

In our particular case, similar laser systems have shown to admit a 3D imbedding presenting horseshoe-type chaos [21]. The fact that our results are fully compatible with this hypothesis reinforces the confidence in the analysis.

Finally, we highlight that braids can be used to analyze dynamical systems admitting a Poincaré section in dimensions higher than 3 [9]. The condition is that the Poincaré map has $k-2$ strongly contracting directions, i.e., that its dynamics can be essentially described by a 2D map, namely the map on the 2D center manifold, irrespective of the dimension $k+1 \geqslant 3$ of the original flow. This result is of a fundamental nature in the sense that general physical systems, regarded as ODE's, could be of very high (and often infinite) dimension.

ACKNOWLEDGMENTS

We thank Robert Gilmore and Gabriel Mindlin for fruitful discussions. Ennio Arimondo (Universitá di Pisa) is gratefully acknowledged for providing the data sets. H.G.S. acknowledges support from Conicet, Fundación Antorchas and the University of Buenos Aires.

[1] P. Boyland, *Braid Types and a Topological Method of Proving Positive Topological Entropy* (Department of Mathematics, Boston University, 1984).
[2] A. Katok, Publ. Math. IHES **51**, 137 (1980).
[3] T. Uezu and Y. Aizawa, Progr. Theor. Phys. **68**, 1907 (1982).
[4] H. G. Solari and R. Gilmore. Phys. Rev. A **37**, 3096 (1988).
[5] J. Birman and R. Williams, Topology **22**, 47 (1983).
[6] G. B. Mindlin, H. G. Solari, M. Natiello, R. Gilmore, and X. Hou, J. Non. Sci. **1**, 147 (1991).
[7] T. Hall, Nonlinearity **7**, 861 (1994).
[8] A. Fathi, F. Laudenbach, and V. Poénaru, *Travaux de Thurston Sur les Surfaces*, Asterisqué 66-67 (Société Mathématique de France, Paris, 1979).
[9] M. A. Natiello and H. G. Solari, J. Knot Theory Ramifications **3**, 511 (1994).
[10] L. H. Kauffman, *Knots and Physics* (World Scientific, Singapore, 1991).
[11] P. Holmes, Archive Rational Mech. Anal. **90**, 115 (1985).
[12] K. Jänlich, *Topology* (Springer-Verlag, Berlin, 1984).
[13] E. Artin, Ann. Math **48**, 101 (1947).
[14] E. N. Lorenz, Technical report, MIT, Boston, 1958, Internal report.
[15] J. Lumley, *Stochastic Tools in Turbulence* (Academic Press, New York, 1970).
[16] N. Aubry, R. Guyonner, and R. Lima, J Nonlin. Sci. **2** (1992).
[17] M. B. Kennel, R. Brown, and H. D. I. Abarbanel, Phys. Rev. A **45**, 3403 (1992).
[18] H. D. I. Abarbanel, R. Brown, J. J. Sidorowich, and L. Sh. Tsimring, Rev. Mod. Phys. **65**, 1331 (1993).
[19] D. P. Lathrop and E. J. Kostelich, in *Measures of Complexity and Chaos*, edited by N. B. Abraham, A. M. Albano, A. Passamante, and P. E. Rapp, Vol. 208 of *NATO Advanced Study Institute Series B: Physics* (Plenum, Berlin, 1989), p. 147.
[20] G. B. Mindlin, R. Lopez-Ruiz, H. G. Solari, and R. Gilmore, Phys. Rev. A **48**, 4297 (1993).
[21] F. Papoff, A. Fioretti, E. Arimondo, G. B. Mindlin H. G. Solari, and R. Gilmore, Phys. Rev. Lett. **68**, 1128 (1991).
[22] G. B. Mindlin and H. G. Solari, Phys. Rev. E **52**, 1497 (1995).